

Research Article

Localized Surface Plasmons Enhanced Light Transmission into c-Silicon Solar Cells

Y. Premkumar Singh,^{1,2} Amit Jain,³ and Avinashi Kapoor¹

¹ Department of Electronic Science, University of Delhi, South Campus, Benito Juarez Road, New Delhi 110021, India

² Department of Physics, Motilal Nehru College, University of Delhi, Benito Juarez Road, New Delhi 110021, India

³ Department of Electronics, Rajdhani College, University of Delhi, Raja Garden, New Delhi 110015, India

Correspondence should be addressed to Avinashi Kapoor; avinashi_kapoor@yahoo.com

Received 30 March 2013; Revised 28 May 2013; Accepted 3 July 2013

Academic Editor: Haricharan S. Reehal

Copyright © 2013 Y. Premkumar Singh et al. This is an open access article distributed under the Creative Commons Attribution License, which permits unrestricted use, distribution, and reproduction in any medium, provided the original work is properly cited.

The paper investigates the light incoupling into c-Si solar cells due to the excitation of localized surface plasmon resonances in periodic metallic nanoparticles by finite-difference time-domain (FDTD) technique. A significant enhancement of AM1.5G solar radiation transmission has been demonstrated by depositing nanoparticles of various metals on the upper surface of a semi-infinite Si substrate. Plasmonic nanostructures located close to the cell surface can scatter incident light efficiently into the cell. Al nanoparticles were found to be superior to Ag, Cu, and Au nanoparticles due to the improved transmission of light over almost the entire solar spectrum and, thus, can be a potential low-cost plasmonic metal for large-scale implementation of solar cells.

1. Introduction

Solar researchers across the globe are showing a keen interest in plasmonic solar cells nowadays. It exploits the nanoscale optical property of noble metals for optical absorption enhancement resulting in an overall increase in the cell conversion efficiency [1–3]. Metallic nanostructures support localized surface plasmon resonances which are the collective oscillations of conduction electrons [2, 3]. Metal nanoparticles strongly scattered the incident light of wavelengths near their resonances, upon excitation. When located in proximity to a high-index substrate, a significant part of the scattered light is coupled into the substrate [1–3]. The resonance wavelength of the nanoparticles can be tuned throughout a broad spectral range by adjusting the size, shape, density, and dielectric properties of the surrounding medium [1–3]. Silver (Ag) and gold (Au) are the most widely used materials for plasmonic solar cells owing to their surface plasmon resonances located in the visible region [2, 3]. Other metals such as aluminium (Al) and copper (Cu) also support surface plasmons whose resonances lie in ultraviolet and visible range of solar spectrum [3].

Several research groups have demonstrated experimentally and numerically the enhancement of optical absorption in Si solar cells using plasmonic particles. Enhanced incoupling of light into semiconductor substrate by scattering from Ag nanoparticles was first recognized in 1998 and 20-fold photocurrent enhancement has been observed on 165 nm thick silicon-on-insulator (SOI) photodetectors at 800 nm wavelength from 100 nm sized Ag particles [4]. In a recent work, an enhancement by a factor of 2.3 in external quantum efficiency of thin Si solar cells at 1100 nm wavelength using Ag nanoparticles was reported [5]. An enhancement of 8.1% in short-circuit current density and an enhancement of 8.3% in energy conversion efficiency were observed using Au nanoparticles on thin a-Si:H p-i-n solar cells [6]. A sevenfold enhancement of light absorption for wafer-based cells at 1200 nm and up to 16-fold enhancement for 1.25 μm thin SOI cells at 1050 nm using Ag nanoparticles were reported [7]. An important role of nanoparticle shape for designing plasmon enhanced solar cells and dependence of scattering cross-section of particle on the distance of the particle from the substrate have been demonstrated [8]. It has been investigated that the contact area between the Ag nanoparticles and the

semiconductor causes a reduced forward scattering but an oxide layer can be used to counteract this reduction [9].

The scattering property of plasmonic nanoparticles is dependent on the shape, size, and surrounding dielectrics [1–3, 5, 8]. It has been demonstrated that spherical-shaped nanoparticles are closer to the ideal shape for efficient light scattering into a substrate, due to their better coupling of the dipolar-like resonance [10, 11]. For efficient scattering of light the size of the nanoparticles should be sufficiently large. When the size is very small, a large amount of light is absorbed by the nanoparticles. Moreover, the size cannot be too large as this leads to multipole oscillations which tend to decrease the scattering efficiency of the nanoparticles [2, 3]. Scattering for nanoparticles around 100 nm is more relevant to solar cell applications [2].

The present work emphasizes the investigation of light coupling into c-Si solar cell by depositing spherical nanoparticles of 100 nm diameter of various metals on the cell surface. Dependence of light transmission and reflection on the spacing of plasmonic particle array has also been investigated.

2. Materials and Method

The basic structure of c-Si solar cell and the computational domain in the present work are shown schematically in Figure 1. The domain consists of a single spherical metal nanoparticle (NP) of 100 nm diameter on the c-Si layer with a 5 nm thin layer of SiO₂ as dielectric spacer. Perfectly matched layers (PMLs) were used in the upper and bottom boundaries to prevent reflection and the Si layer was extended into the PML to make it appear semi-infinite. Periodical boundary conditions (PBCs) were used in the lateral directions to model periodic array of nanoparticles. A plane wave source of X-polarized electric-field was placed 500 nm above the Si surface. The transmitted power into the solar cell was measured by a frequency-domain monitor placed at the plane of interface between the Si and SiO₂ layers [11–13]. It was calculated by integrating the poynting vector of the Fourier-transformed electromagnetic fields over the plane in the normal direction. The reflection monitor was located 100 nm behind the source. Integrated transmission efficiency (ITE) or integrated reflection efficiency (IRE) within the spectral range of 300–1100 nm was calculated as

$$\text{ITE or IRE} = \frac{\int_{300}^{1100} (\lambda/hc) [T(\lambda) \text{ or } R(\lambda)] S(\lambda) d\lambda}{\int_{300}^{1100} (\lambda/hc) S(\lambda) d\lambda}, \quad (1)$$

where λ is the wavelength of light in free space, h is Planck's constant, c is the speed of light in free space, $T(\lambda)$ or $R(\lambda)$ is the transmittance or reflectance of light, and $S(\lambda)$ is the irradiance spectrum of AM1.5G.

Finite-difference time-domain (FDTD) technique was adopted for numerical simulations [14]. MIT Electromagnetic Equation Propagation (MEEP), a free, open-source simulation software package, was used for all the FDTD calculations in this study [15]. FDTD is a widely used technique for computational electromagnetism in which space is divided into a regular discrete grid and then the E and H

TABLE I: Values of the parameters used in the material models.

	Ag	Au	Al	Cu	c-Si	SiO ₂
ω_p (eV)	9.01	9.03	14.98	10.83		
σ_0	0.845	0.760	0.575	0.523		
γ_0 (eV)	0.048	0.053	0.047	0.030		
ω_1 (eV)	0.816	0.415	0.162	0.291	4.344	0.057
σ_1	0.065	0.024	0.227	0.061	10.835	0.829
γ_1 (eV)	3.886	0.241	0.333	0.378	0.199	0.199
ω_2 (eV)	4.481	0.830	1.544	2.957		0.099
σ_2	0.124	0.010	0.052	0.104		0.095
γ_2 (eV)	0.452	0.345	0.312	1.056		0.199
ω_3 (eV)	8.185	2.969	1.808	5.300		13.387
σ_3	0.011	0.071	0.166	0.723		1.098
γ_3 (eV)	0.065	0.870	1.351	3.213		0.199
ω_4 (eV)	9.083	4.304	3.473	11.18		
σ_4	0.840	0.601	0.030	0.638		
γ_4 (eV)	0.916	2.494	3.382	4.305		
ϵ_∞					1.035	1

fields are evolved in discrete time steps. The discretization of both space and time should be sufficiently fine to approximate for true continuous equations. A number of simulations were run with decreasing grid size until a convergent solution was obtained. Grid size in the entire computational domain was 2.5 nm for all the calculations. Even mirror symmetry along X-direction was used to reduce the computation time. In our calculations, besides the two commonly used plasmonic metals Ag and Au, the low-cost metals Al and Cu are also chosen. Optical constants for various metals were taken from [16] and data for c-Si and SiO₂ were taken from [17].

The Drude-Lorentz equation for metals can be written as

$$\epsilon(\omega) = 1 - \frac{\sigma_0 \omega_p^2}{\omega(\omega - i\gamma_0)} + \sum_{j=1}^k \frac{\sigma_j \omega_p^2}{(\omega_j^2 - \omega^2) + i\omega\gamma_j}. \quad (2)$$

The Lorentz equation for c-Si and SiO₂ is

$$\epsilon(\omega) = \epsilon_\infty + \sum_{j=1}^k \frac{\sigma_j \omega_j^2}{\omega_j^2 - \omega^2 - i\omega\gamma_j}, \quad (3)$$

where $\epsilon(\omega)$ is the dielectric function; ω_p is the plasma frequency with oscillator strength σ_0 and damping frequency γ_0 ; k is the number of oscillators with resonant frequency ω_j , strength σ_j , and damping frequency γ_j ; and ϵ_∞ is the infinite frequency dielectric response. These equations were used with the parameters given in Table I.

3. Results and Discussion

Figure 2 shows the transmission (a) and reflection (b) spectra of a periodic array of spherical Ag nanoparticles of diameter (D) 100 nm at various spacing (S). The spectrum without nanoparticles as a reference is also included. Note that spacing is measured from the center of the particles. In Figure 2(a), the transmission of light into the Si substrate in

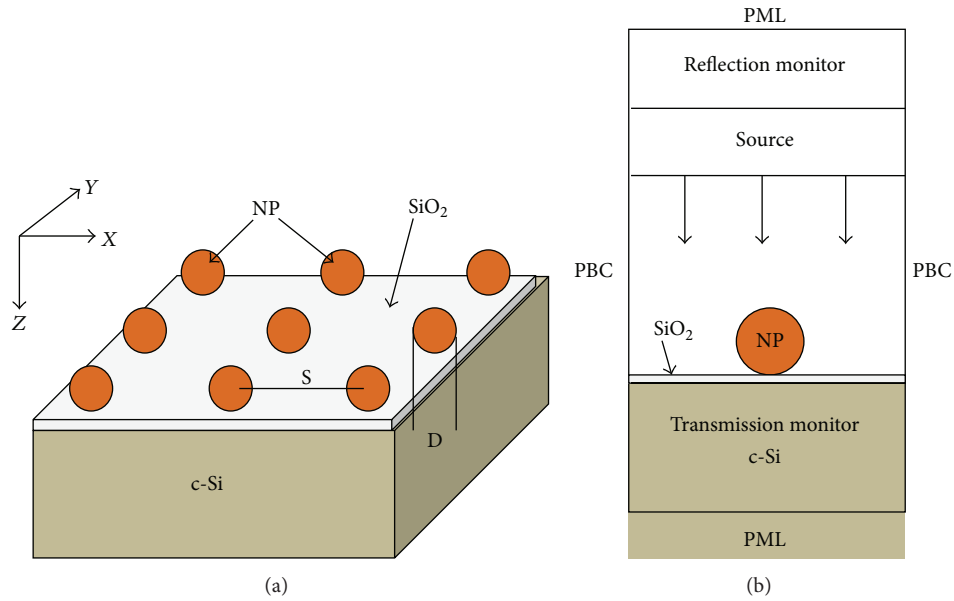


FIGURE 1: (a) Basic structure of c-Si solar cell under investigation. (b) Schematic of the computational domain used for FDTD simulations.

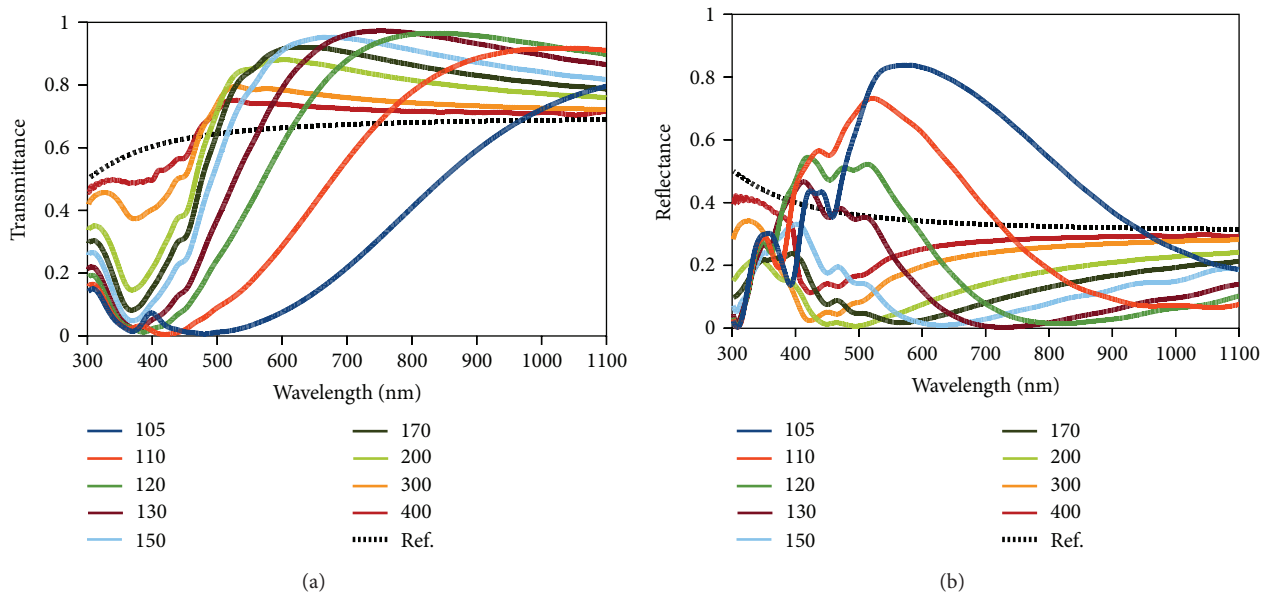


FIGURE 2: Transmission (a) and reflection (b) spectra of spherical Ag nanoparticles of 100 nm diameter at various spacing (in nm).

spectral range above resonance wavelength is enhanced by the presence of the nanoparticles. The mechanism behind this effect is the constructive interference between the forward scattered light by nanoparticles and the incident light [5, 11]. However, transmission decreased dramatically at wavelengths below resonance. This reduction occurs due to a Fano effect, that is, a destructive interference between scattered and incident light occurring below resonance wavelength [5, 11]. The strength of coupling between surface plasmons of metallic nanoparticles depends on the particle spacing.

For closely spaced particles, a strong coupling causes a broadening of plasmon resonance and a large nonradiative loss [18]. Increasing the spacing causes a decoupling of metallic nanoparticles and in turn weakens the nonradiative loss. Therefore, light transmission increases with increasing the spacing from 105 nm to 150 nm. However, upon a further increase in the spacing from 150 nm to 400 nm, transmission decreases. If the spacing is extremely large, the effect of nanoparticles can be almost negligible and the structure converges to the case with no nanoparticles. We can also

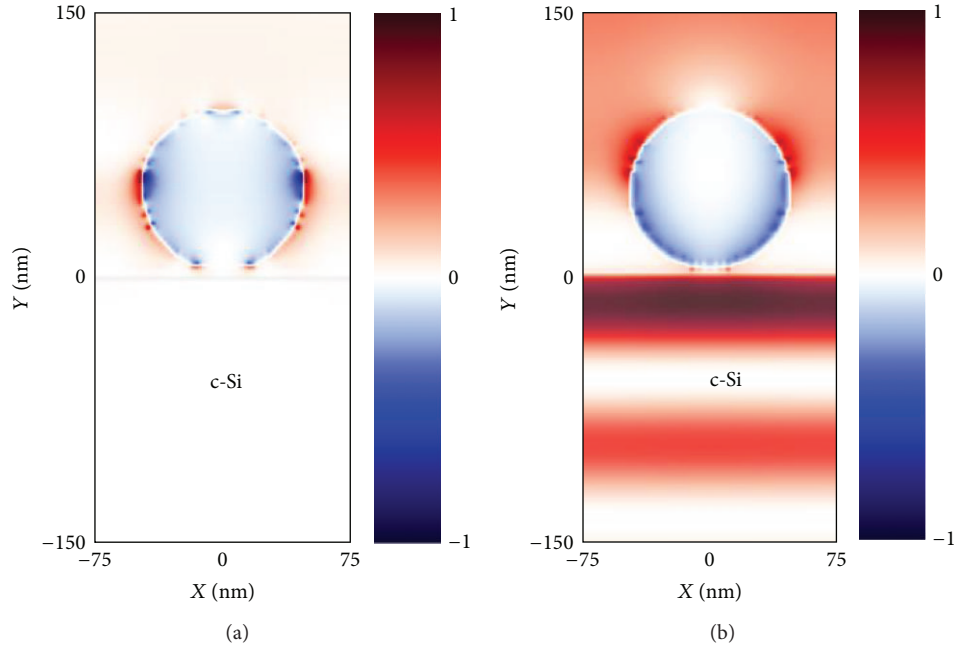


FIGURE 3: Spatial distribution of electric-field energy density of Ag nanoparticles at 150 nm spacing under different wavelengths illumination: (a) 370 nm and (b) 670 nm.

observe a remarkable blueshift of the resonance wavelength as the spacing increases and this is consistent with previously reported result [19]. Enhancement in transmission can be credited to reduced reflection of the Si substrate after depositing the nanoparticles. Reflected power decreased significantly with increasing interparticle spacing from 105 nm to 150 nm and then increased as spacing is increased up to 400 nm (Figure 2(b)). The reduced reflection is due to intrinsic absorption of nanoparticles and forward scattering by nanoparticles into the Si substrate. The dips at shorter wavelengths in both the transmission and reflection spectra indicate light absorbed by the nanoparticles. The suppressed reflection at longer wavelength would lead directly to an increase in transmission. Figure 3 shows the spatial distribution of electric-field energy density with Ag nanosphere at 150 nm spacing under the illumination of minimum (a) and maximum (b) transmission wavelengths. The transmission enhancement can be attributed to the excited surface plasmon resonance and a significant field enhancement is observed at both sides of the nanoparticle.

Figure 4 shows the transmission (a) and reflection (b) spectra of spherical nanoparticles of $D = 100$ nm and $S = 150$ nm for various metals. A substantial loss in transmitted power at shorter wavelengths is observed with Ag, Cu, and Au nanoparticles since their localized surface plasmon resonances are located in visible range where solar spectrum is still very intense. On the other hand, Al nanoparticles showed enhanced transmission of light over almost the entire solar spectrum, since their plasmon resonances lie in ultraviolet region, resulting in a significant reduction in loss [13, 20, 21]. At higher wavelengths, Ag, Au, and Cu have very similar optical properties and have a slightly

greater transmitted power than Al nanoparticles. This is due to the weak interband transition of Al nanoparticles at around 825 nm [22]. In Figure 4(b), the reduced reflection of light at the shorter wavelengths indicates that Au, and Cu nanoparticles absorbed a large portion of the incident light. Figure 5 shows the values of ITE (a) and IRE (b) with nanoparticles of various metals as a function of spacing. The ITE curves sharply increase to their peak values at $S = 150$ nm and decay slowly with increasing the spacing. Reflection power decreases significantly due to the presence of nanoparticles, and IRE curves have minimum values at around $S = 150$ nm. These relationships show that reduced reflection induced the increase in transmission. Interestingly, Al nanoparticles have 84% of ITE and 9% of IRE at 150 nm spacing which again shows 7% of incident light is absorbed by nanoparticles. These results demonstrate that amongst various metals under investigation, Al is the best choice of plasmonic material for solar cell applications.

4. Conclusion

An enhancement in transmission of AM1.5G solar radiation into a semi-infinite c-Si substrate has been demonstrated by depositing spherical nanoparticles of various metals on the upper surface. The existence of a transmission maximum is the effect of light scattering by the nanoparticles into the Si substrate. Spacing-dependent wavelength integrated transmission and reflection efficiencies have been studied. Amongst various metals under investigation, Al nanoparticles tend to provide the best performance due to a broadband light coupling enhancement, matching the solar spectrum.

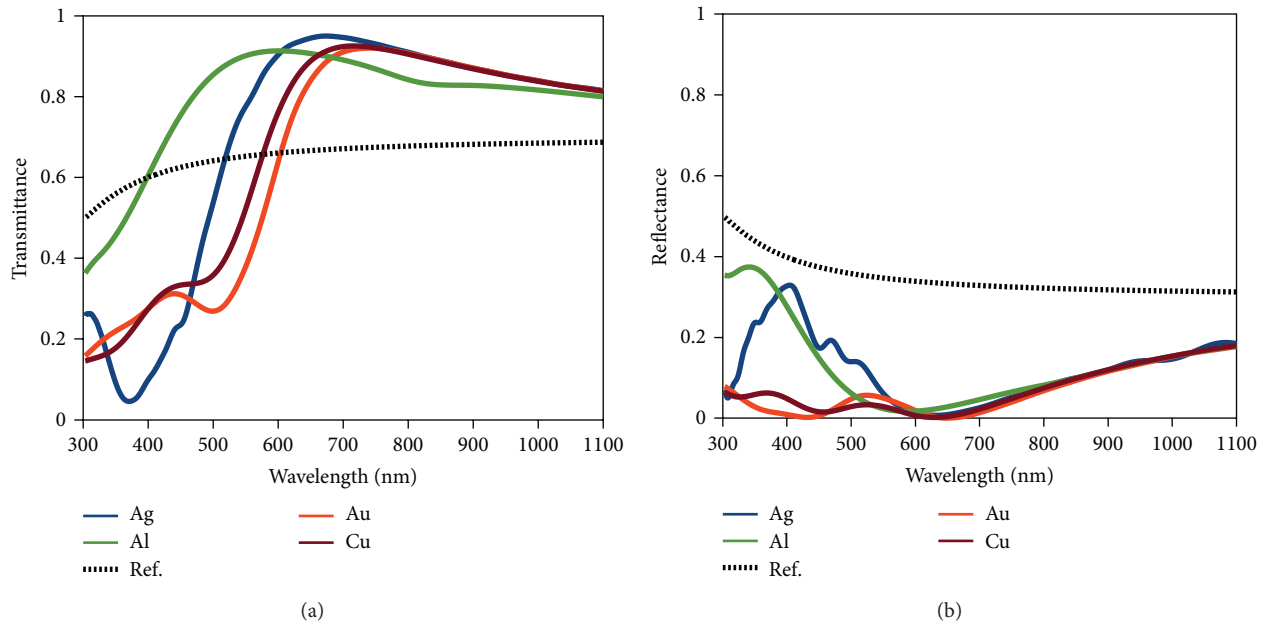


FIGURE 4: Transmission (a) and reflection (b) spectra of spherical nanoparticles of 100 nm diameter at 150 nm spacing for various metals.

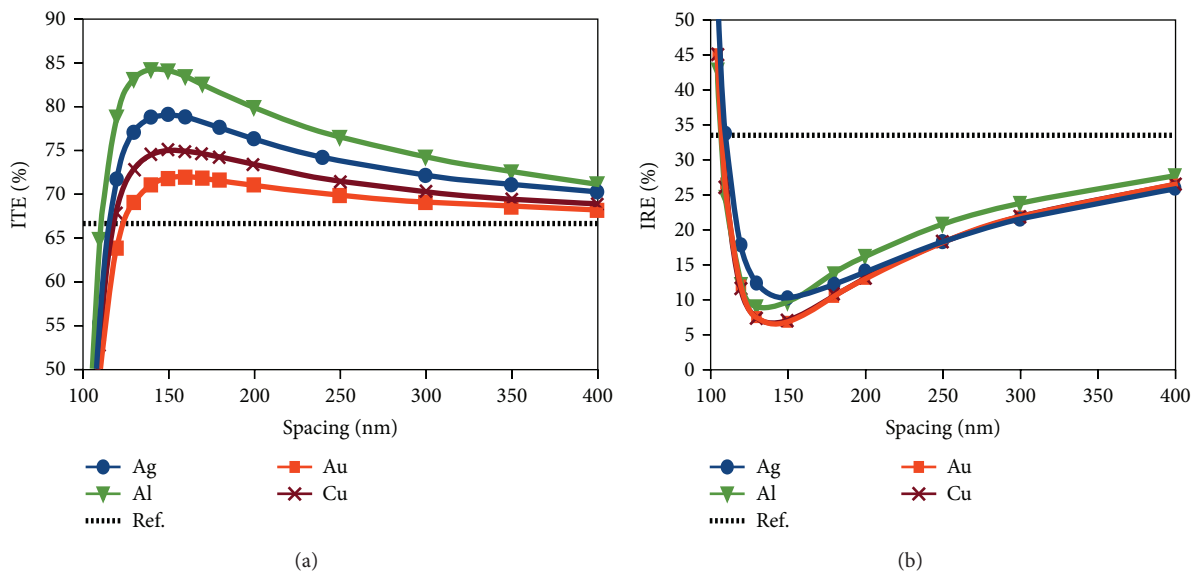


FIGURE 5: Values of ITE (a) and IRE (b) of spherical nanoparticles of 100 nm diameter of various metals as a function of spacing.

Thus, low-cost and earth abundant Al has the potential for large-scale implementation of plasmonic nanoparticles and hence enhanced solar cell performance.

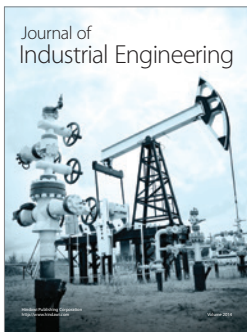
Conflict of Interests

The authors confirm that this paper content has no conflict of interest.

References

- [1] H. A. Atwater and A. Polman, "Plasmonics for improved photovoltaic devices," *Nature Materials*, vol. 9, no. 3, pp. 205–213, 2010.
- [2] S. Pillai and M. A. Green, "Plasmonics for photovoltaic applications," *Solar Energy Materials and Solar Cells*, vol. 94, no. 9, pp. 1481–1486, 2010.
- [3] K. R. Catchpole and A. Polman, "Plasmonic solar cells," *Optics Express*, vol. 16, no. 26, pp. 21793–21800, 2008.

- [4] H. R. Stuart and D. G. Hall, "Island size effects in nanoparticle-enhanced photodetectors," *Applied Physics Letters*, vol. 73, no. 26, pp. 3815–3817, 1998.
- [5] F. J. Beck, A. Polman, and K. R. Catchpole, "Tunable light trapping for solar cells using localized surface plasmons," *Journal of Applied Physics*, vol. 105, no. 11, Article ID 114310, 7 pages, 2009.
- [6] D. Derkacs, S. H. Lim, P. Matheu, W. Mar, and E. T. Yu, "Improved performance of amorphous silicon solar cells via scattering from surface plasmon polaritons in nearby metallic nanoparticles," *Applied Physics Letters*, vol. 89, no. 9, Article ID 093103, 3 pages, 2006.
- [7] S. Pillai, K. R. Catchpole, T. Trupke, and M. A. Green, "Surface plasmon enhanced silicon solar cells," *Journal of Applied Physics*, vol. 101, no. 9, Article ID 093105, 8 pages, 2007.
- [8] K. R. Catchpole and A. Polman, "Design principles for particle plasmon enhanced solar cells," *Applied Physics Letters*, vol. 93, no. 19, Article ID 191113, 3 pages, 2008.
- [9] A. Centeno, J. Breeze, B. Ahmed, H. Reehal, and N. Alford, "Scattering of light into silicon by spherical and hemispherical silver nanoparticles," *Optics Letters*, vol. 35, no. 1, pp. 76–78, 2010.
- [10] C. Hagglund, M. Zach, G. Petersson, and B. Kasemo, "Electromagnetic coupling of light into a silicon solar cell by nanodisk plasmons," *Applied Physics Letters*, vol. 92, no. 5, Article ID 053110, 3 pages, 2008.
- [11] P. Spinelli, C. V. Lare, E. Verhagen, and A. Polman, "Controlling Fano lineshapes in plasmon-mediated light coupling into a substrate," *Optics Express*, vol. 19, no. S3, pp. A303–A311, 2011.
- [12] P. Spinelli, M. Hebbink, R. de Waele, L. Black, F. Lenzmann, and A. Polman, "Optical impedance matching using coupled plasmonic nanoparticle arrays," *Nano Letters*, vol. 11, no. 4, pp. 1760–1765, 2011.
- [13] Y. Zhang, Z. Ouyang, N. Strokes, B. Jia, Z. Shi, and M. Gu, "Low cost and high performance Al nanoparticles for broadband light trapping in Si wafer solar cells," *Applied Physics Letters*, vol. 100, no. 15, Article ID 151101, 4 pages, 2012.
- [14] A. Taflov and S. C. Hagness, *Computational Electrodynamics: The Finite-Difference Time Domain Method*, Artech House, Norwood, Mass, USA, 2nd edition, 2000.
- [15] A. F. Oskooi, D. Roundy, M. Ibanescu, P. Bermel, J. D. Joannopoulos, and S. G. Johnson, "Meep: a flexible free-software package for electromagnetic simulations by the FDTD method," *Computer Physics Communications*, vol. 181, no. 3, pp. 687–702, 2010.
- [16] A. D. Rakić, A. B. Djurišić, J. M. Elazar, and M. L. Majewski, "Optical properties of metallic films for vertical-cavity optoelectronic devices," *Applied Optics*, vol. 37, no. 22, pp. 5271–5283, 1998.
- [17] E. D. Palik, *Handbook of Optical Constants of Solid*, Academic Press, San Diego, CA, USA, 1998.
- [18] C. Rockstuhl, S. Fahr, and F. Lederer, "Absorption enhancement in solar cells by localized plasmon polaritons," *Journal of Applied Physics*, vol. 104, no. 12, Article ID 123102, 7 pages, 2008.
- [19] W. Rechberger, A. Hohenau, A. Leitner, J. R. Krenn, B. Lamprecht, and F. R. Aussenegg, "Optical properties of two interacting gold nanoparticles," *Optics Communications*, vol. 220, no. 1–3, pp. 137–141, 2003.
- [20] Y. A. Akimov and W. S. Koh, "Resonant and nonresonant plasmonic nanoparticle enhancement for thin-film silicon solar cells," *Nanotechnology*, vol. 21, no. 23, Article ID 235201, 2010.
- [21] T. F. Villesen, C. Uhrenfeldt, B. Johansen, J. L. Hansen, H. U. Ulriksen, and A. N. Larsen, "Aluminium nanoparticles for plasmon-improved coupling of light into silicon," *Nanotechnology*, vol. 23, no. 8, Article ID 085202, 2012.
- [22] C. Langhammer, M. Schwind, B. Kasemo, and I. Zoric, "Localized surface plasmon resonances in aluminium nanodisks," *Nano Letters*, vol. 8, no. 5, pp. 1461–1471, 2008.



Hindawi

Submit your manuscripts at
<http://www.hindawi.com>

